Available online at www.sciencedirect.com
SCIENCE DIRECT®
Biochimica et Biophysica Acta 1618 (2003) 25–32
BIOCHIMICA ET BIOPHYSICA ACTA
BBA
www.bba-direct.com

Proteorhodopsin in living color: diversity of spectral properties within living bacterial cells

Bradley R. Kelemen, Mai Du, Rasmus B. Jensen*

Genencor International, Inc., 925 Page Mill Road, Palo Alto, CA 94304 USA

Received 24 July 2003; received in revised form 25 September 2003; accepted 3 October 2003

Abstract

Proteorhodopsin is a family of over 50 proteins that provide phototrophic capability to marine bacteria by acting as light-powered proton pumps. The potential importance of proteorhodopsin to global ocean ecosystems and the possible applications of proteorhodopsin in optical data storage and optical signal processing have spurred diverse research in this new family of proteins. We show that proteorhodopsin expressed in *Escherichia coli* is functional and properly inserted in the membrane. At high expression levels, it appears to self-associate. We present a method for determining spectral properties of proteorhodopsin in intact *E. coli* cells that matches results obtained with detergent-solubilized, purified proteins. Using this method, we observe distinctly different spectra for protonated and deprotonated forms of 21 natural proteorhodopsin proteins in intact *E. coli* cells. Upon protonation, the wavelength maxima red shifts between 13 and 53 nm. We find that pK_a values between 7.1 and 8.5 describe the pH-dependent spectral shift for all of the 21 natural variants of proteorhodopsin. The wavelength maxima of the deprotonated forms of the 21 natural proteorhodopsins cluster in two sequence-related groups: blue proteorhodopsins (B-PR) and green proteorhodopsins (G-PR). The site-directed substitution Leu105Gln in Bac31A8 proteorhodopsin shifts this G-PR's wavelength maximum to a wavelength maximum the same as that of the B-PR Hot75m1 proteorhodopsin. The site-directed substitution Gln107Leu in Hot75m1 proteorhodopsin shifts this B-PR's wavelength maximum to a wavelength maximum as that of Bac31A8 proteorhodopsin.

Keywords: Halophilic archaebacteria; Proteorhodopsin; *Escherichia coli*

1. Introduction

Proteorhodopsin (PR) is a recently identified family of proteins analogous to the light-powered, proton pump bacteriorhodopsin (BR) from halophilic archaebacteria [1]. Active research on BR has been ongoing for three decades. Moreover, there has been an interest in using BR in bioelectronic device applications [2–5].

PR was identified by sequencing DNA isolated from uncultivated, marine eubacteria [1,6,7]. PR is capable of light-driven proton pumping with a photocycle faster than that of sensory rhodopsins; therefore, PR was reported to be part of a phototropic pathway like BR [1,6–13]. Proteorhodopsin-containing marine bacteria are distributed globally throughout the oceans and more than 50 genes of the PR family have been identified to date [1,6,7].

The PR family members are all highly homologous between themselves (77–99% sequence identity) but show less sequence homology to BR (~ 22% sequence identity), archaeal sensory rhodopsins (~ 14% sequence identity) and halorhodopsins (14–24% sequence identity). The family of PR differs from BR in both spectral character as well as the pH dependence of the spectral characteristics [8,10,12–15]. A red-shift of the visible spectra of PR with protonation can be described by a pK_a in the neutral to slightly basic range, while a similar shift in BR is only seen in extremely acidic conditions [16,17].

Nine members of the PR family have been characterized spectroscopically previously [1,6,7]. From the analysis of these family members, PR can be divided into two groups: blue PR (B-PR) and green PR (G-PR). These two groups have distinctly different absorbance maxima (G-PR near 520 nm and B-PR at 490 nm). The first PR to be described [1], Bac31A8 PR, is an example of a G-PR, while the variant Hot75m1 PR is an example of a B-PR. The color tuning of these proteins is thought to be optimized to match the light that reaches the depth at which the bacteria thrive [6,7].

Abbreviations: PR, proteorhodopsin; BR, bacteriorhodopsin

* Corresponding author. Tel.: +1-650-846-4048; fax: +1-650-621-8048.
E-mail address: rjensen@genencor.com (R.B. Jensen).

0005-2736/$ - see front matter © 2003 Elsevier B.V. All rights reserved.
doi:10.1016/j.bbamem.2003.10.002

Here, we describe a method to analyze the spectral properties of a protein within intact bacterial cells. We characterize, within intact bacterial cells, 21 natural PRs with respect to their spectral properties and the pK_a values that describe the pH dependence of their spectra. From this data and sequence alignment, we also divide PR into two groups distinguished by the spectral characteristics of their deprotonated forms. A single amino acid substitution accounts for the majority of the spectral difference between these two groups of PR.

2. Materials and methods

2.1. Cloning and expression of natural PR variants

A total of 21 natural proteorhodopsin genes were PCR amplified from plasmids containing the cloned genes (obtained from E. DeLong, Monterey Bay Aquarium Research Institute [1,6]) using the PR-u4 (5′-AAATTATTACTGATATTAGGTAGTG-3′) and PR-d2 (5′-AGCATTAGAAGATTCTTTAACAGC-3′) primers and cloned into *Escherichia coli* using the pTrcHis2 TOPO TA Expression Kit (Invitrogen, Carlsbad, CA). Proteorhodopsins expressed from these constructs contain C-terminal myc- and his-tags.

BL21-Codonplus-RIL cells (Stratagene, La Jolla, CA) containing the proteorhodopsin expression plasmids were grown in 200 ml LB + 0.5% glucose + 100 μg/ml carbenicillin + 10 μM all-trans-retinal medium at 37 °C. Proteorhodopsin expression was induced by adding 0.5 mM IPTG + 10 μM all-trans-retinal and the cultures were incubated for additional 4 h at 37 °C. The cells were harvested by centrifugation at 3500 × *g* for 10 min and stored at − 80 °C.

2.2. Proteorhodopsin purification

Cells were suspended in lysis buffer containing 40 mM MOPS (pH 7.0), 20 mM $MgCl_2$, 0.2 mg/ml lysozyme, 0.2 mg/ml DNAseI, 2% dodecyl-β-D-maltoside (DβM), and protease inhibitors (Complete, EDTA-free Protease Inhibitor Cocktail Tablets from Roche Applied Science, Indianapolis, IN) and lysed at 0 °C by sonication. The lysates were incubated with His-Tag affinity resin in Talon spin columns (Clontech, Palo Alto, CA) that had been equilibrated with 1 ml wash buffer containing 40 mM MOPS (pH 7.0) and 0.5% DβM. The resin was washed three times with 1 ml wash buffer containing 40 mM MOPS (pH 7.0) and 0.5% DβM. Proteorhodopsins were eluted from the resin two times with 0.5 ml elution buffer containing 40 mM MOPS (pH 7.0), 0.5% DβM and 250 mM EDTA. The two elutates were pooled and EDTA was removed by three successive 10-fold concentrations using a Microcon YM-10 centrifugal filter unit (Millipore, Billerica, MA) and dilutions with a buffer contained 40 mM MOPS (pH 7.0). The proteorhodopsin samples were then concentrated 10-fold and stored at 4 °C.

2.3. Microscopy

Cells for immunofluorescence microscopy were grown as described above. Low- and high-level proteorhodopsin-expressing cells were grown without or with IPTG induction, respectively. An approximately 10-fold increase of PR is expected with IPTG induction. The cells were fixed using 3% formaldehyde + 0.015% glutaraldehyde or methanol directly in the growth medium. The fixation solution was removed by filtration. Immunofluorescence microscopy was performed essentially as described [18]. Cells were permeabilized using 20 μg/ml lysozyme. Monoclonal anti-C-myc antibodies (Sigma-Aldrich, St. Louis, MO) were used at a 1:500 dilution and Alexa-488-labeled secondary antibodies (Molecular Probes, Eugene, OR) were used at a 1:200 dilution. Images were processed using Photoshop (Adobe Systems Incorporated, San Jose, CA).

2.4. Site-directed mutagenesis of PR

PR genes were mutagenized using the QuickChange Site-Directed Mutagenesis Kit (Stratagene) as described by the manufacturer. The primers used to construct the L105Q Bac31A8 mutant was 5′-TTGGTTACTAACAGTTCCTC**TAc**AAATATGTGAATTCTACTTAAT-3′ and 5′-ATTAAGTAGAATTCACATATTT**gTA**GAGGGAACTGTTAGTAACCAA-3′ and for Q107L Hot75m1 5′-GTTATTAACTGTTCCATTA**CtA**ATGGTTTGAGTTCTATCTAATTCT-3′ and 5′-AGAATTAGATAGAACTCAACCAT**TaG**TAATGGAACAGTTAATAAC-3′. Bold letters indicate the codon that was mutated, lowercase letters indicate nucleotides that were changed compared to the wild-type sequence.

2.5. Spectroscopy of turbid samples

Cells (6 ml) were grown for 6 h as described without induction by IPTG. The cells were collected by centrifugation at 4500 × *g* for 6 min and suspended in 5 ml sterile water. A 900 μl sample of cells was added to a 100 μl aliquot of concentrated buffer (1.0 M acetate (pH 4.9), 1.0 M MES (pH 5.8), 1.0 M MOPS (pH 6.7), 1.0 M TAPS (pH 8.1), or 1.0 M CHES (pH 9.1)). To test the correlation of absorbance with protein concentration in our system, varying aliquots (2, 4, 8 or 16 μl) of a 10 mg/ml sample of BR were added to cells expressing the LacZ control protein.

The spectra of the 21 natural PR were measured in intact cells at five different extracellular pH values using a modular, easily configurable spectrophotometer (OLIS RSM-100, On-Line Instrument Systems, Inc., Bogart, GA) adapted for use with turbid samples. In this configuration, the photomultiplier tube detector (PMT) was placed adjacent to the sample cuvette and the PMT voltage was

adjusted to be optimal for each cell dilution. The absorption from a strain containing a control plasmid (pTrcHis2–LacZ) was subtracted from PR-containing samples. To correct for differences in background light scattering caused by variations in cell densities between the sample and the reference, a linear baseline determined by least-squares fitting of the first 10 (396–404 nm) and last 10 wavelength (616–625 nm) and absorbance values in each spectrum was subtracted. The spectra were then adjusted to the same minimum value by subtracting the differences in minimum values.

2.6. pK_a value determination

To determine the pK_a value describing the pH-dependent spectral change, the adjusted absorbance intensities at each wavelength and pH were fitted to Eq. (1) by least-squares regression analysis using the Solver function of Microsoft Excel.

$$\mathrm{Abs} = \mathrm{Abs}_{\mathrm{acidic}} + \mathrm{Abs}_{\mathrm{basic-acidic}} \times (10^{\mathrm{pH}-\mathrm{p}K_{\mathrm{rh}}}) \quad (1)$$

Different values of the absorbance of the acidic form $\mathrm{Abs}_{\mathrm{acidic}}$ and the difference spectrum between the basic and the acidic forms $\mathrm{Abs}_{\mathrm{basic-acidic}}$ were fitted at each wavelength, but the same value of pK_a was fitted for data at all wavelengths. The values $\mathrm{Abs}_{\mathrm{acidic}}$ and $\mathrm{Abs}_{\mathrm{basic-acidic}}$ were used to reconstruct wavelength spectra for acidic and basic forms of PR and from this data the wavelength maxima at acidic and basic pH were determined (Table 1).

Table 1
The values of the pK_a of a pH-dependent change in spectral properties, wavelength maxima and the family grouping of proteorhodopsin variants[a]

Proteorhodopsin	pK_a	Basic max (nm)	Acidic max (nm)	Family[b]
Bac31A8	7.6 (7.1)[c]	521 (517)[c]	538 (543)[c]	G
Bac40E8	7.7	519	538	G
Bac64A5	7.6	519	538	G
Hot0m1	8.0	518	538	G
Hot75m1	8.2 (8.4)[c]	493 (504)[c]	546 (538)[c]	B
Hot75m3	7.2	488	538	B
Hot75m4	7.6	490	538	B
Hot75m8	8.0	493	538	B
MB0m1	7.9	518	540	G
MB0m2	7.9	523	540	G
MB20m2	7.9	523	538	G
MB20m5	8.2	526	569	G
MB20m12	7.6	524	540	G
MB40m1	7.7	519	538	G
MB40m5	8.5	525	558	G
MB40m12	7.5	523	536	G
MB100m5	7.8	523	538	G
MB100m7	8.1	524	550	G
MB100m9	7.3	524	538	G
MB100m10	7.7	524	538	G
PalE6	7.1	490	542	B
Bac31A8 L105Q	8.3	493	535	G → B
Hot75m1 Q107L	7.9	512	559	B → G

[a] Wavelength maxima were determined from spectra of proteorhodopsins in the membrane of whole cells using a spectrophotometer modified to measure absorbance of turbid samples. Values of pK_a were determined by the global fit of entire spectra collected at five different pH values. See text for details.

[b] Family is either blue (B) or green (G) and refers to both sequence alignment and spectral character at basic pH.

[c] Values given in parenthesis were determined using solubilized, purified proteins in buffers of different pH values. See text for details.

2.7. Spectroscopy of purified PR

Purified PR (5 μl of 10 mg/ml) was diluted in 500 μl of buffer containing 100 mM either citrate (pH 3.54, 3.97, 4.50, or 5.03), acetate (pH 4.88), MES (pH 5.34, 5.80, or 6.35), MOPS (pH 6.75 or 7.32), TAPS (pH 7.91 or 8.43), CHES (pH 9.00 or 9.50), or CAPS (10.12 or 10.64). Wavelength spectra from 250 to 650 nm were obtained on a Cary3 spectrophotometer (Varian Inc., Palo Alto, CA). The pK_a value describing the pH-dependent spectral shift was calculated using Eq. (1) as described previously.

3. Results

3.1. Cellular localization of PR

To confirm that PR is incorporated into the cell membrane and to determine its cellular localization pattern when expressed in the heterologous host *E. coli*, we performed immunofluorescence staining of PR-expressing cells using antibodies reactive with the myc-tag of the recombinant PR. No staining was observed with cells that do not express PR (data not shown), showing that the signal is specific to PR. We analyzed the protein localization at both low (Fig. 1A) and high (Fig. 1B) levels of PR expression. As shown in Fig. 1, PR appears in a typical membrane localization pattern at both expression levels. The protein does not appear as inactive protein in inclusion bodies, even at the high expression level, a common problem with over-expression of membrane proteins [19]. This conclusion is supported by the observations that PR forms a proper chromophore with added all-trans-retinal, is capable of proton pumping, PR fractionates with the membrane components, PR can be solubilized using mild detergents and the PR localization pattern is different from a typical inclusion body localization pattern. At low levels of protein expression, PR has a diffuse membrane localization pattern (Fig. 1A). The PR protein appears to be more abundant at the center of the cells with slight exclusion from the polar regions. In contrast, PR localization is more punctate and less diffuse at high expression levels (Fig. 1B), indicating that some degree of PR molecule self-association takes place at these conditions. However, the staining pattern seen for high levels of PR expression is not consistent with the existence of large PR patches similar to the BR-containing purple membrane of *Halobacterium salinarum* [20], indicating that only small, if any, two-dimensional crystalline structures exist when PR is expressed in *E. coli*.

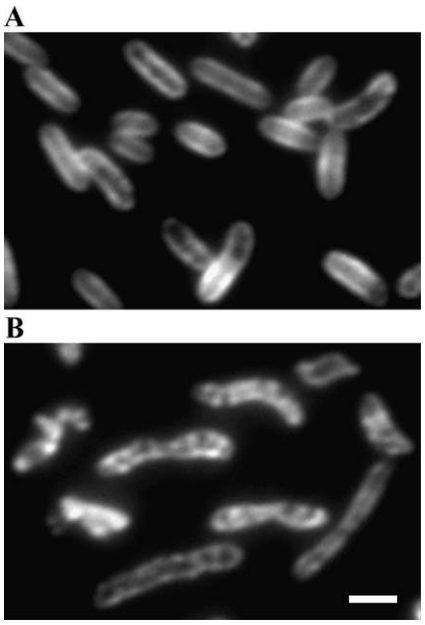

Fig. 1. Membrane localization of proteorhodopsin at low and high levels of expression. Immunofluorescence microscopy of *E. coli* cells expressing proteorhodopsin. (A) Even membrane localization of proteorhodopsin at low level of protein expression. (B) Punctate membrane localization at high level of protein expression (scale bar is 2 μm).

3.2. Spectra in turbid samples

To determine if spectral properties of PR variants could be directly studied in intact cells, we modified an OLIS RSM-100 spectrophotometer to allow for measurements of turbid samples. We placed the photomultiplier tube adjacent to the sample holder to allow for detection of more of the scattered light passing though the sample. The use of an appropriate blank consisting of cells with similar scattering properties and setting the photomultiplier tube voltage for each different cell density proved to be very important. To establish that measurements made on the instrument are linear with respect to concentration of chromophore, we added increasing concentrations of BR to a turbid cell sample and measured the resulting spectra. Fig. 2A shows the increasing absorbance spectra and Fig. 2B shows the increase of absorbance at 565 nm with increasing BR concentration. The absorbance intensity and concentration values correlate linearly providing confidence in a method to directly measure PR spectral properties in intact cells.

The measurement of the wavelength spectra of Hot75m1 PR in intact *E. coli* cells at different extracellular pH values is shown in Fig. 3A. Hot75m1 PR has an absorbance maximum at 546 nm at acidic conditions and at 493 nm at basic conditions. As a comparison to the proteins in intact cells, we measured the spectra of detergent solubilized, purified PR. Fig. 3B shows the spectra of solubilized, purified Hot75m1 PR in acidic and basic buffers as well as in buffers close to the pK_a of Hot75m1 PR. Similar spectral properties were observed in the both samples, confirming the validity of the measure of PR spectral properties in intact cells.

3.3. Value of the pK_a describing the pH-dependent spectral change

The spectra of Hot75m1 PR, both purified and in intact cell membrane, in a number of buffers spanning the pK_a of the pH-dependent spectral change of PR are presented as an example of the isosbestic point observed in the titration data (Fig. 3A and B). The spectra of PR in both cases are broadened at pH values near its pK_a because the spectra are a combination of the spectra of acidic and basic forms. These data are fit to Eq. (1) with a value of the pK_a of the titratable group responsible for the spectral shift of Hot75m1 PR of 8.2 in intact cells and 8.4 for purified protein. Using the method described above, we measured the spectral

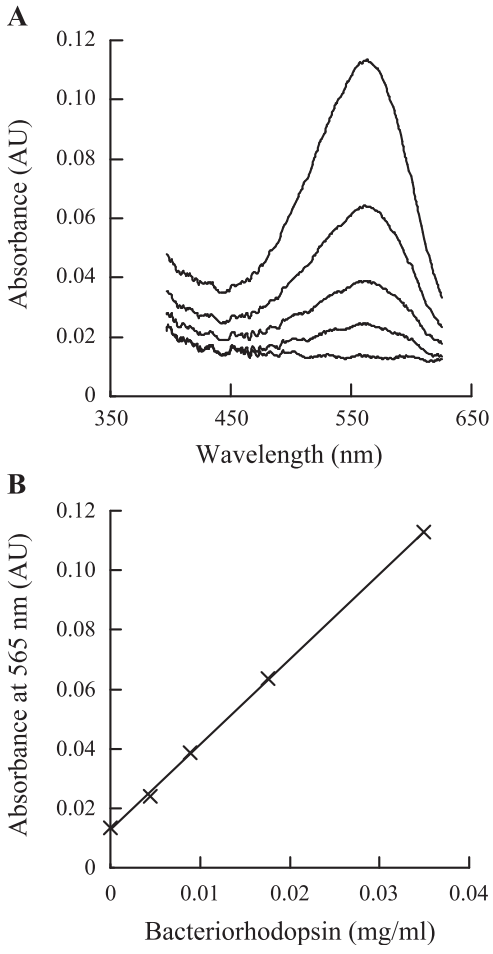

Fig. 2. Visible wavelength spectra of bacteriorhodopsin in turbid samples. (A) The spectra of bacteriorhodopsin (in ascending order, 0.035, 0.018, 0.009, and 0.004 mg/ml) added to a slurry of *E. coli* cells (OD_{600} of 2.0) expressing a control protein (LacZ) were collected on an OLIS RSM-100 spectrophotometer modified to measure turbid samples (see text for details). (B) Absorbance intensity measured at 565 nm is linearly proportional (R^2>0.99) to the concentration of the bacteriorhodopsin in the sample.

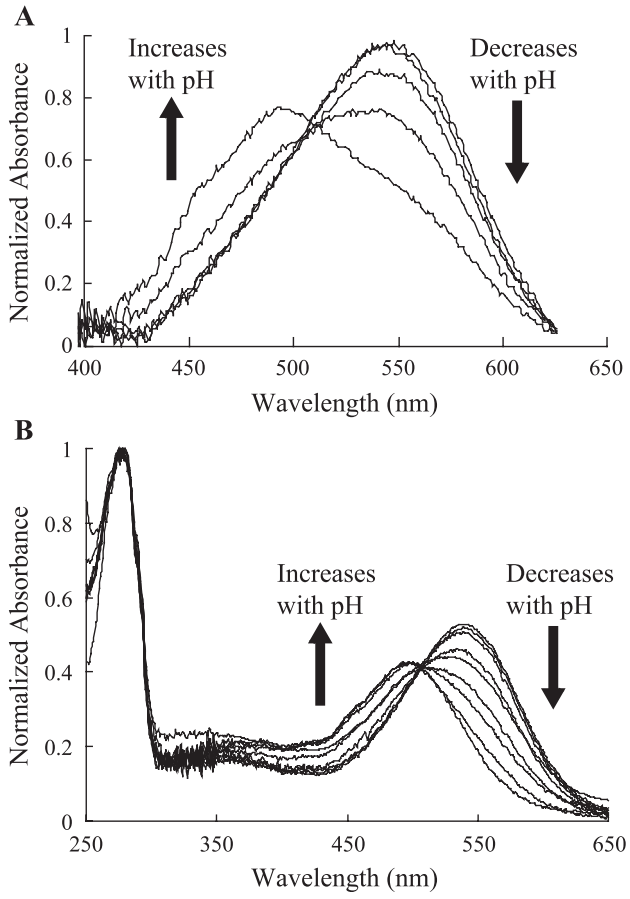

Fig. 3. Spectral properties of proteorhodopsin. (A) The absorbance spectra of Hot75m1 proteorhodopsin in the membrane of intact *E. coli* cells suspended in various buffers (pH 4.9, 6.0, 6.9, 8.1, and 9.1) are dependent on the extracellular pH. Arrows indicate changes in spectra with increasing pH. (B) The absorbance spectra of detergent solubilized, purified Hot75m1 proteorhodopsin suspended in various buffers (pH 4.0, 4.9, 6.4, 7.3, 7.9, 8.4, 9.0, 9.5 and 10.6) are dependent on buffer pH. Arrows indicate changes in spectra with increasing pH.

properties of 21 natural PR variants at a pH range of 4.9–9.1 in intact cells. The results of this analysis are summarized in Table 1 along with values of two purified proteins presented in parenthesis for comparison. The values of pK_a determined for all PR variants evenly span a range from 7.1 to 8.5. The spectra of all PR shift to the red with decreasing extracellular pH.

3.4. Spectral characteristics of 21 natural PR variants

The data presented in Fig. 4 show the distribution of values of the wavelength maxima for acidic and basic forms of PR (see also Table 1). The values of wavelength maxima of acidic forms of PR span a range from 536 to 569 nm without any isolated groups of data. The values of wavelength maxima for basic forms of PR separate into two isolated groups, one between 488 and 493 nm (B-PR) and another group between 518 and 526 nm (G-PR). These two groups of data correlate with the separation of two genetically related groups.

3.5. Tuning of the spectral properties of PR

The two groups, B-PR and G-PR, can be separated from one another purely by sequence comparison [6]. Of the differences within primary PR sequences, we identified, by sequence comparison with BR, an amino acid position Leu105 in Bac31A8 PR (Gln107 in Hot75m1 PR) that appears to be close to the retinal cofactor and thus likely to impact the spectra of PR. All G-PR have Leu at this position, and all B-PR have Gln at this position. We constructed a variant of the G-PR Bac31A8 PR with Leu105 replaced by Gln and a corresponding variant in the B-PR Hot75m1 PR with Gln107 replaced by Leu. The site-directed variant Leu105Gln Bac31A8 PR (Fig. 5, dashed red line) has a spectrum similar to that of Hot75m1

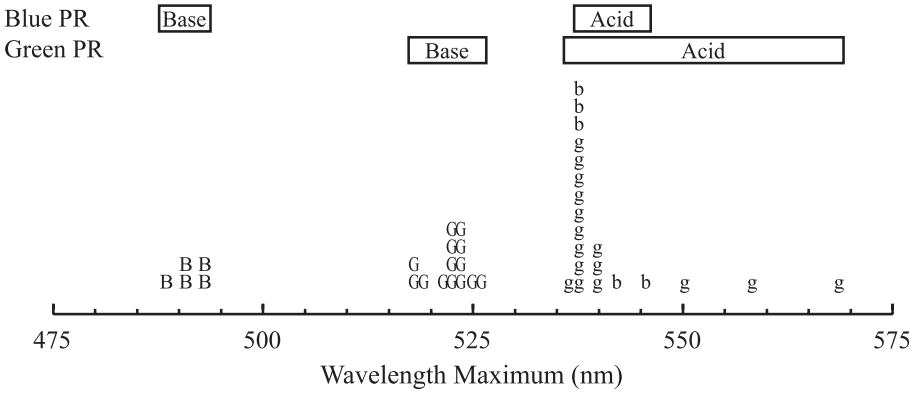

Fig. 4. Two groups of proteorhodopsins, blue and green, are distinguished by spectral properties at basic pH but not at acidic pH. The line graph shows the wavelength maximum values of blue proteorhodopsins (at acidic pH (b) and basic pH (B)) and green proteorhodopsins (at acidic pH (g) and basic pH (G)). The boxes above the graph summarize the distribution of wavelength maxima of the members of the two PR families at acidic and basic conditions. The wavelength maximum values for the two groups overlap at acidic pH, yet show two distinct groups of values at basic pH.

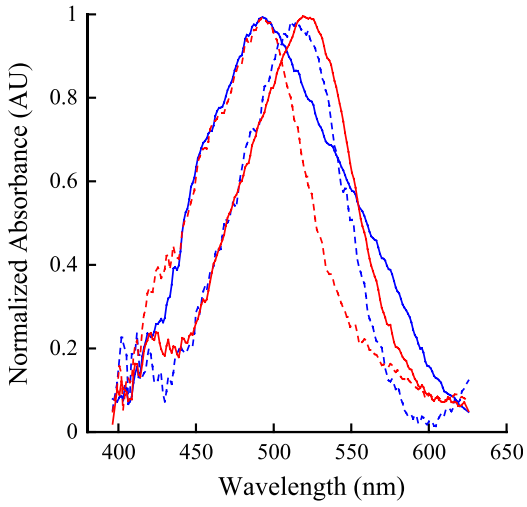

Fig. 5. Spectral tuning of the proteorhodopsin family. Absorbance spectra of PR variants show the importance of position L105 (Q107) to PR spectral properties. The absorbance spectrum of Bac31A8 proteorhodopsin (solid red line) is similar to the absorbance spectrum of Q107L Hot75m1 proteorhodopsin (dashed blue line). The absorbance spectrum of Hot75m1 proteorhodopsin (solid blue line) is similar to the spectrum of L105Q Bac31A8 proteorhodopsin (dashed red line).

PR (solid blue line). Correspondingly, the site-directed variant Gln107Leu Hot75m1 PR (dashed red line) has a spectrum similar to that of Bac31A8 PR (see also Table 1). These data confirm the significance of position 105 to the absorbance spectra of PR.

4. Discussion

We describe a method to determine the spectral properties of PR, and potentially any other protein with a visible wavelength chromophore, within intact bacterial cells. We show that 21 naturally occurring and two site-directed variants of PR have a red-shifting spectral transition describable by a single protonation event with a pK_a value within one unit of 7.5. We also show that spectral variability in the deprotonated, active forms of PR divide into two genetically distinct groups G-PR and B-PR with a single site, position 105, providing most of the difference in spectra.

4.1. Expression of PR in E. coli

Unlike BR [21, 22], PR can be functionally expressed in *E. coli* with the exogenous addition of all-trans-retinal [1]. This expression may be possible because of a greater similarity of the natural PR producing cells with *E. coli* than the BR producing halophillic archeabacterium. The possibility remains that the membrane of *E. coli* may not be an ideal environment for PR. Nonetheless, the ability to easily manipulate PR genes in *E. coli* along with the existing body of knowledge about BR will expedite research of this recently discovered form of bacterial proton pump. The natural diversity of the PR family may also provide insight not available with BR. The inability to express fully functional BR in a bacterial system capable of rapid high-level protein production, limited availability of genetic systems for strain and protein manipulation and poor compatibility of *H. salinarum* with true high-throughput screening systems has slowed modification of BR to obtain the protein properties required for commercial applications [2]. The optoelectronic and biotechnological applications proposed for BR [2–5] like optical data storage, optical filtering and artificial retinas might be realized by the use of PR.

4.2. Cellular localization of PR

An immunofluorescence microscopy analysis of fixed PR-expressing cells show that PR localizes to the membrane (Fig. 1), indicating proper expression and assembly in the membrane without formation of inclusion bodies containing aggregated inactive protein. At a low level of protein expression, PR appears smoothly distributed in the cell membrane but seems enriched at the center of the cell and diminished at the poles of the cell. This localization pattern may be due to different lipid composition, different protein composition or different curvature of the membrane of the poles and centers of cells [23,24]. At a high expression level, PR appears to be located in the membrane, but in brighter spots isolated from one another. This indicates that PR molecules self-associate at high expression levels. In *H. salinarum*, a threshold concentration of BR is required for formation of purple membrane patches containing two-dimensional crystalline arrays of BR and large patches are only observed at the highest BR expression levels [25,26]. Thus, at a low level of PR expression in *E. coli*, the protein concentration could be below a threshold required for self-association. The punctate distribution of PR at the high expression level could indicate the formation of small patches of PR. The PR expression level used in this work might not be sufficient to form large patches similar to the BR patches observed in *H. salinarum*. It is unknown if PR expressed in *E. coli* form crystalline protein–lipid arrays as observed with BR patches in *H. salinarum*. The microscopy method used here does not have sufficient resolution to detect crystalline protein–lipid array formation.

4.3. Spectra of bacterial rhodopsins in turbid samples

We developed a system to measure the spectral properties of PR in intact cells to facilitate the analysis of the large number of naturally occurring PRs. To verify our in-cell spectroscopy method, we collected spectral data of BR diluted into a suspension of *E. coli* cells using a modified OLIS RSM-100 spectrophotometer. The spectra of BR shown in Fig. 2A indicate that the chromophore of BR can be distinguished from the other possible cellular chromophores. The comparison of absolute absorbance values to

the concentration of BR (Fig. 2B) indicates that our system follows Beer's law for absorbance and is not dominated by light scattering. The existence of isosbestic points in the titration data of whole cells indicate that we are measuring a single titration event in much the way we would with purified protein (compare Fig. 3A and B). Also, the similarity of pK_a and absorbance maxima values from the titration of samples of purified protein and titration of protein within whole cells is an indication of the validity of our method of spectroscopy of turbid samples (see Table 1). The method we describe could be used for bacteriorhodopsin and other chromophoric proteins either membrane bound or cytoplasmic.

Previously, Martinez and Turner [27] described a whole cell paste reflection spectroscopy method for high-throughput screening of spectral properties of bacteriorhodopsin mutants. Their method requires a larger volume of cells than our method and lyses the cells, disrupting the natural membrane environment of the proteins, whereas our method retains the membrane intact.

4.4. pK_a and spectral change

All of the 23 variants of PR that we studied showed a pH-dependent change in spectral character that could be described by a single protonation event with a value of pK_a between 7.1 and 8.5. Since we observe the titration with intact cells, the titration site must be accessible from the outside of the cells. The observed spectral change is an indication of the protonation state of the retinal cofactor or residues located close to it. Dioumaev et al. [8] showed that a Asp97Asn Bac31A8 mutant did not undergo a pH-dependent shift in spectral character. This strongly indicates that the titration event we observe is that of Asp97. Recently, it was described that two titratable groups control the pH-dependent change in spectral character in the B-PR Hot75m4 [13]. However, we do not have evidence for two titratable groups in Hot75m4 and three other natural B-PR variants both in intact cells and with purified proteins. The different observations might be caused by the different fitting methods used. For example, we performed global fitting using the entire absorbance spectra, whereas Wang et al. [13] used the λ_{max} of the spectra.

4.5. Spectral properties of PR variants

Red shifted spectra of Bac31A8 PR at acidic conditions have previously been observed [8,10]. We have extended this observation for 21 natural PRs, showing that the pH-dependent switch in spectral properties is a general property of the PR family. There exist a similar, roughly 35 nm, separation of extremes within the pool of acidic spectra (wavelength maxima from 536 to 569 nm) and basic spectra (wavelength maxima from 488 to 526 nm). However, the basic spectra separate into two distinct groups that correlate with genetic differences [6].

The existence of two pH-dependent spectral forms causes a broadening of spectra at a pH close to the value of the pK_a. The mixture of the two forms produces an additive spectrum that is broader than spectra at either pH extreme. Additionally, the acidic and basic forms of PR have different photocycles, with the most important difference being the absence of a M-like intermediate and proton pumping at low pH [8,11,12,14]. This indicates that materials containing PR will need to be kept at an extreme pH to reduce the impact of the other spectral form.

There exist two main genetic groups of PR, G-PR and B-PR, that correlate with the wavelength maxima at basic pH. We have shown that the distinction of the two families can be explained almost completely by a single amino acid difference, Leu105 in Bac31A8 and Gln107 in Hot75m1. This residue position is likely part of the retinal binding-site. There may be other sites that impact the diversity of PR spectral properties, however, this site appears to be the major determinant of spectral tuning of the PR family. Similar results with other PR variants were recently described [7]. The L105 residue does not appear to control the acidic spectrum.

A greater spread of the absorbance maxima was observed with the acidic spectra than the basic spectra. The difference in the acidic spectra of outlying members (such as MB40m5 PR) may reflect the diversity of the PR family. Alternatively, it may arise from mutations introduced during the PCR cloning of the PR genes from seawater samples [6] and may not be representative of the PR natural diversity. Since we base our conclusions from results obtained for a large sample of PR genes, we feel that our conclusions are representative of natural PR diversity.

The deprotonated form of PR is the active, proton-pumping state of the protein [8,10,12,14]. In a natural seawater environment, the pH is generally between 7.5 and 8.1 [28]. Since the environmental pH is close to the pK_a of all of the PR family members characterized here, a significant proportion of the PR protein in the natural environment will be in the non-proton pumping acidic form. Having a significant fraction of protein in a non-functioning state would be inefficient, leading to loss of significant amounts of light energy. Perhaps, the cells expressing PR use this pK_a in a regulatory mechanism. Alternatively, cells expressing PR may maintain a local pH at the membrane that is distinctly more basic than seawater. Perhaps, the efficiency of proton pumping improves if the proton transfer groups along the pumping pathway have pK_a values close to the ambient pH. However, the pK_a of the similar transition in BR is several pH values below the environmental pH value of BR's natural habitat salt marshes [16,17]. The reason that PRs have pK_a values so close to ambient pH is a perplexing issue that might provide important information about the mechanism of proton pumping by PR and the biology of phototrophy in the oceans.

Even though there is spectral diversity in the whole PR family, there exists less spectral diversity of proteorhodopsin

in its active, deprotonated form than in the protonated and deprotonated forms of the proteins. Most of the functional spectral diversity can be accounted for by the difference in polarity or size of a single amino acid residue in the retinal binding pocket.

Acknowledgements

We thank Roopa Ghimikar, Gregg Whited and Sang-Kyu Lee for critical reading of the manuscript. The work was supported as part of the Silicon Biotechnology™ Alliance partnership between Dow Coring Corporation and Genencor International Inc.

References

[1] O. Beja, L. Aravind, E.V. Koonin, M.T. Suzuki, A. Hadd, L.P. Jovanovich, S.B. Jovanovich, C.M. Gates, R.A. Feldman, J.L. Spudich, E.N. Spudich, E.F. DeLong, Bacterial rhodopsin: evidence for a new type of phototrophy in the sea, Science 289 (2000) 1902–1906.

[2] K.J. Wise, N.B. Gillespie, J.A. Stuart, M.P. Krebs, R.R. Birge, Optimization of bacteriorhodopsin for bioelectronic devices, Trends Biotechnol. 20 (2002) 387–394.

[3] J. Min, H.G. Choi, B.K. Oh, W.H. Lee, S.H. Paek, J.W. Choi, Visual information processing using bacteriorhodopsin-based complex LB films, Biosens. Bioelectron. 16 (2001) 917–923.

[4] N. Hampp, Bacteriorhodopsin as a photochromic retinal protein for optical memories, Chem. Rev. 100 (2000) 1755–1776.

[5] N.A. Hampp, Bacteriorhodopsin: mutating a biomaterial into an optoelectronic material, Appl. Microbiol. Biotechnol. 53 (2000) 633–639.

[6] O. Beja, E.N. Spudich, J.L. Spudich, M. Leclerc, E.F. DeLong, Proteorhodopsin phototrophy in the ocean, Nature 411 (2001) 786–789.

[7] D. Man, W. Wang, G. Sabehi, L. Aravind, A.F. Post, R. Massana, E.N. Spudich, J.L. Spudich, O. Beja, Diversification and spectral tuning in marine proteorhodopsins, EMBO J. 22 (2003) 1725–1731.

[8] A.K. Dioumaev, L.S. Brown, J. Shih, E.N. Spudich, J.L. Spudich, J.K. Lanyi, Proton transfers in the photochemical reaction cycle of proteorhodopsin, Biochemistry 41 (2002) 5348–5358.

[9] R.A. Krebs, U. Alexiev, R. Partha, A. DeVita, M.S. Braiman, Detection of fast light-activated H+ release and M intermediate formation from proteorhodopsin, BMC Physiol. 2 (2002) 5.

[10] T. Friedrich, S. Geibel, R. Kalmbach, I. Chizhov, K. Ataka, J. Heberle, M. Engelhard, E. Bamberg, Proteorhodopsin is a light-driven proton pump with variable vectoriality, J. Mol. Biol. 321 (2002) 821–838.

[11] G. Varo, L.S. Brown, M. Lakatos, J.K. Lanyi, Characterization of the photochemical reaction cycle of proteorhodopsin, Biophys. J. 84 (2003) 1202–1207.

[12] A.K. Dioumaev, J.M. Wang, Z. Bálint, G. Váró, J.K. Lanyi, Proton transport by proteorhodopsin requires that the retinal Schiff base counterion Asp-97 be anionic, Biochemistry 42 (2003) 6582–6587.

[13] W.W. Wang, O.A. Sineshchekov, E.N. Spudich, J.L. Spudich, Spectroscopic and photochemical characterization of a deep ocean proteorhodopsin, J. Biol. Chem. 278 (2003) 33985–33991.

[14] M. Lakatos, J.K. Lanyi, J. Szakacs, G. Varo, The photochemical reaction cycle of proteorhodopsin at low pH, Biophys. J. 84 (2003) 3252–3256.

[15] R.A. Krebs, D. Dunmire, R. Partha, M.S. Braiman, Resonance Raman characterization of proteorhodopsin's chromophore environment, J. Phys. Chem., B 107 (2003) 7877–7883.

[16] P.C. Mowery, R.H. Lozier, Q. Chae, Y.W. Tseng, M. Taylor, W. Stoeckenius, Effect of acid pH on the absorption spectra and photoreactions of bacteriorhodopsin, Biochemistry 18 (1979) 4100–4107.

[17] S.P. Balashov, E.S. Imasheva, R. Govindjee, T.G. Ebrey, Titration of aspartate-85 in bacteriorhodopsin: what it says about chromophore isomerization and proton release, Biophys. J. 70 (1996) 473–481.

[18] I.J. Domian, K.C. Quon, L. Shapiro, Cell type-specific phosphorylation and proteolysis of a transcriptional regulator controls the G1-to-S transition in a bacterial cell cycle, Cell 90 (1997) 415–424.

[19] R. Grisshammer, C.G. Tate, Overexpression of integral membrane proteins for structural studies, Q. Rev. Biophys. 28 (1995) 315–422.

[20] R. Henderson, The purple membrane from *Halobacterium halobium*, Annu. Rev. Biophys. Bioeng. 6 (1977) 87–109.

[21] R.J. Dunn, N.R. Hackett, J.M. McCoy, B.H. Chao, K. Kimura, H.G. Khorana, Structure–function studies on bacteriorhodopsin: I. Expression of the bacterio-opsin gene in *Escherichia coli*, J. Biol. Chem. 262 (1987) 9246–9254.

[22] I.P. Hohenfeld, A.A. Wegener, M. Engelhard, Purification of histidine tagged bacteriorhodopsin, pharaonis halorhodopsin and pharaonis sensory rhodopsin II functionally expressed in *Escherichia coli*, FEBS Lett. 442 (1999) 198–202.

[23] E. Mileykovskaya, W. Dowhan, Visualization of phospholipid domains in *Escherichia coli* by using the cardiolipin-specific fluorescent dye 10-*N*-nonyl acridine orange, J. Bacteriol. 182 (2000) 1172–1175.

[24] C.M. Koppelman, T. Den Blaauwen, M.C. Duursma, R.M. Heeren, N. Nanninga, *Escherichia coli* minicell membranes are enriched in cardiolipin, J. Bacteriol. 183 (2001) 6144–6147.

[25] D.C. Neugebauer, H.P. Zingsheim, D. Oesterhelt, Biogenesis of purple membrane in halobacteria, Methods Enzymol. 97 (1983) 218–226.

[26] T.A. Isenbarger, M.P. Krebs, Role of helix–helix interactions in assembly of the bacteriorhodopsin lattice, Biochemistry 38 (1999) 9023–9030.

[27] L.C. Martinez, G.J. Turner, High-throughput screening of bacteriorhodopsin mutants in whole cell pastes, Biochim. Biophys. Acta 1564 (2002) 91–98.

[28] T. Clayton, R.H. Byrne, Spectrophotometric seawater pH measurements: total hydrogen ion concentration scale calibration of m-cresol purple and at-sea results, Deep-Sea Res. 40 (1993) 2115–2129.